The results of our numerical experiments give values from three to ten times this value. Some of this difference is due to the lack of deeper mantle flow, and some of it is due to the weakness of the temperature dependence (our highest A is still about a factor of two too small), which creates a strong downwelling curtain leading to large negative topography and geoid. This curtain is the result of mechanical thinning and would be much smaller at Earth-like values of A.

The range of buoyancy fluxes in our experiments (calculated from the rate at which topography is created) is 0.8 to 10.7×10^6 g s^{-1}, which includes the estimated value for the Hawaiian swell. As demonstrated in (*17*), the plume buoyancy flux is smaller than the buoyancy flux measured from the topography, because of the buoyancy flux of the downwelling curtain. The buoyancy flux does not obey a simple scaling with either A or T_p, because of competition between mechanical thinning, spreading of plume material within the asthenosphere, and thinning by small-scale instabilities. Experiments to control these factors individually should be designed.

We have demonstrated that the small-scale instabilities that promote lithospheric thinning are initiated when the excess temperature of the plume is about twice $\Delta T_{\mathrm{rheol}}$, independent of A. This finding gives us confidence in extrapolating to Earth-like values of A, which require only modest plume temperatures ($T_p > 100$ K) to produce small-scale convective flows.

REFERENCES AND NOTES

1. R. S. Dietz and H. W. Menard, *J. Geol.* **61**, 99 (1953).
2. S. T. Crough and G. A. Thompson, *Earth Planet. Sci. Lett.* **31**, 397 (1976).
3. R. S. Detrick and S. T. Crough, *J. Geophys. Res.* **83**, 1236 (1978).
4. S. T. Crough, *Geophys. J. R. Astron. Soc.* **55**, 451 (1978).
5. D. T. Sandwell, *J. Geophys. Res.* **87**, 1001 (1982); T. Spohn and G. Schubert, *Tectonophysics* **94**, 67 (1983); A. O. Gliko, *Izvest. Acad. Sci. USSR* **22**, 257 (1986); G. M. Liu and C. G. Chase, *J. Geophys. Res.* **94**, 5571 (1989).
6. L. Fleitout, C. Froidevaux, D. Yuen, *Tectonophysics* **132**, 271 (1986).
7. L. Fleitout and D. A. Yuen, *J. Geophys. Res.* **89**, 9227 (1984); D. A. Yuen and L. Fleitout, *Nature* **313**, 125 (1985).
8. R. W. Griffiths and I. H. Campbell, *J. Geophys. Res.* **96**, 18295 (1991).
9. H. C. Nataf and F. M. Richter, *Phys. Earth Planet. Inter.* **29**, 320 (1982); F. M. Richter, H. C. Nataf, S. F. Daly, *J. Fluid Mech.* **129**, 173 (1983); A. Davaille and C. Jaupart, *J. Geophys. Res.* **99**, 19853 (1994).
10. ———, *J. Fluid Mech.* **253**, 141 (1993).
11. S. Morris and D. Canright, *Phys. Earth Planet. Inter.* **36**, 35 (1984); A. C. Fowler, *Stud. Appl. Math.* **72**, 189 (1985); E. F. Fishbein, thesis, University of California, Los Angeles (1988).
12. R. P. Von Herzen *et al.*, *J. Geophys. Res.* **87**, 6711 (1982).
13. R. P. Von Herzen, M. J. Cordery, R. S. Detrick, C. Fang, *ibid.* **94**, 13783 (1989).
14. N. H. Sleep, *ibid.* **99**, 9327 (1994); J. Phipps-Morgan, W. J. Morgan, E. Price, *ibid.* **100**, 8045 (1995); N. M. Ribe, *ibid.* **101**, 16195 (1996); N. H. Sleep, *ibid.*, p. 28065.
15. M. T. Woods and E. A. Okal, *Geophys. J. Int.* **125**, 325 (1996).
16. M. Monnereau, M. Rabinowicz, E. Arquis, *J. Geophys. Res.* **98**, 809 (1993).
17. N. M. Ribe and U. R. Christensen, *ibid.* **99**, 669 (1994).
18. P. J. Tackley, thesis, California Institute of Technology, Pasadena (1994); *J. Geophys. Res.* **101**, 3311 (1996).
19. G. F. Davies, *J. Geophys. Res.* **93**, 10467 (1988); N. H. Sleep, *ibid.* **95**, 6715 (1990).
20. E. M. Robinson, B. Parsons, S. F. Daly, *Earth Planet. Sci. Lett.* **82**, 335 (1987); E. M. Robinson and B. Parsons, *J. Geophys. Res.* **93**, 3469 (1988).
21. E. Takahashi, *J. Geophys. Res.* **91**, 9367 (1986); F. J. Zhang and C. Herzberg, *ibid.* **99**, 17729 (1994).
22. J. G. Caldwell and D. L. Turcotte, *ibid.* **84**, 7572 (1979).
23. R. S. Borch and H. W. Green, *Phys. Earth Planet. Inter.* **55**, 269 (1989).
24. P. E. van Keken and C. W. Gable, *J. Geophys. Res.* **100**, 20291 (1995).
25. F. M. Richter, *ibid.* **78**, 8735 (1973).
26. F. H. Busse and J. A. Whitehead, *J. Fluid Mech.* **47**, 305 (1971).

27. We thank the three reviewers for their insightful comments. This research was partially funded by NASA grants NAG54628 and NAG53863.

14 October 1997; accepted 12 January 1997

Photometry and Spectroscopy of the GRB 970508 Optical Counterpart

Alberto J. Castro-Tirado, Javier Gorosabel, Narciso Benítez, Christian Wolf, Ralf Fockenbrock, Enrique Martínez-González, Helmuth Kristen, Adrick Broeils, Holger Pedersen, Jochen Greiner, Enrico Costa, Marco Feroci, Luigi Piro, Filippo Frontera, Luciano Nicastro, Eliana Palazzi, Corrado Bartolini, Adriano Guarnieri, Nicola Masetti, Adalberto Piccioni, Marco Mignoli, Magrethe Wold, Mark Lacy, Kurt Birkle, Tom Broadhurst, Søren Brandt, Niels Lund

An optical transient within the error box of the gamma ray burst GRB 970508 was imaged 4 hours after the event. It displayed a strong ultraviolet excess, and reached maximum brightness 2 days later. The optical spectra did not show any emission lines, and no variations on time scales of minutes were observed for 1 hour during the decline phase. According to the fireball and afterglow models, the intensity should rise monotonically before the observed optical maximum, but the data indicate that another physical mechanism may be responsible for the constant phase seen during the first hours after the burst.

Gamma ray bursts (GRBs), brief flashes of cosmic high-energy photons, remain one of the most elusive mysteries for high-energy astrophysicists (*1*), mainly because we do not know how far away they are. The finding of counterparts—transient emissions released at other wavelengths after the bursts—is needed to help explain their origin. Since the advent of the Italian-Dutch x-ray satellite BeppoSAX in April 1996 (*2*), it has been possible to perform deep multiwavelength searches just a few hours after an event, allowing the detection of counterparts associated with the GRBs.

On 8 May 1997, 21:41:45 UT, GRB 970508 was detected by the gamma ray burst monitor (*3*) and the wide-field camera (*4*) of BeppoSAX. The single-peaked GRB lasted 15 s, and its position (*5*) was further refined to a radius of 3 arc min (*6*). This event was also observed as a rather weak GRB by the Burst and Transient Source Experiment (BATSE) on the Compton Gamma-Ray Observatory. The duration was about 35 s, with a single main pulse lasting 3.6 s, reaching a peak flux (50 to 300 keV) of $\sim 2 \times 10^{-10}$ J m^{-2} s^{-1}. The gamma ray fluence (flux integrated over time) was $\sim 1.6 \times 10^{-9}$ J m^{-2} (*7*). After 5.7 hours, BeppoSAX was reoriented toward the burst location, and an x-ray source was detected within the region of uncertainty given by the less accurate GRB localization (the error box) (*8*).

We obtained unfiltered and R-band images with the Calar Alto Faint Object Spectrograph at the 2.2-m telescope of the German-Spanish Calar Alto Observatory (CAHA), beginning 4 hours and 6 min after the GRB (9 May, 1:48 UT). The 2048×2048 pixel charge-coupled device (CCD) frames with scale 0.53 arc sec per pixel provided a circular field (16 arc min in diameter), which was centered on the initial GRB location. We also obtained a mosaic of images with the 4.2-m William Herschel Telescope (WHT) on La Palma (Canary Islands), starting 4 hours and 24 min after the event. The position of the x-ray source was imaged (300-s exposure) by the

Table 1. Journal of the GRB 970508 observations (photometry). The telescope name is preceded by its aperture in meters.

Date of 1997	Time (UT)	Telescope	Filter	Integration time (s)	Magnitude
09 May	01:48	2.2 CAHA	–	600	21.2 ± 0.1
09 May	02:06	4.2 WHT	U	300	20.3 ± 0.3
09 May	03:04	2.2 CAHA	R	300	21.2 ± 0.1
09 May	21:35	2.2 CAHA	R	600	20.9 ± 0.1
10 May	01:21	4.2 WHT	U	1200	19.9 ± 0.3
10 May	20:24	1.5 Loiano	R	1200	19.8 ± 0.1
10 May	20:55	2.2 CAHA	R	60	19.8 ± 0.2
11 May	02:13	4.2 WHT	U	1200	19.6 ± 0.3
11 May	03:27	4.2 WHT	R	600	20.1 ± 0.1
11 May	20:50	2.2 CAHA	R	300	20.4 ± 0.1
12 May	01:38	4.2 WHT	U	1200	19.9 ± 0.3
12 May	02:32	4.2 WHT	U	1200	20.0 ± 0.3
12 May	03:20	2.2 CAHA	R	180	20.5 ± 0.1
12 May	05:20	4.2 WHT	B	40 × 60	21.5 ± 0.3
13 May	20:24	1.5 Loiano	R	3600	20.5 ± 0.1
14 May	20:38	1.5 Loiano	R	3600	21.5 ± 0.2
15 May	01:55	2.5 NOT	U	1200	22.0 ± 0.5
25 August	22:27	4.2 WHT	U	2 × 2700	≥23.0
26 August	00:00	4.2 WHT	R	3 × 900	≥24.0

primary focus camera through a wide U-band filter (*9*) on 9 May, 02:06 UT. The 2048 × 2048 pixel CCD frames (0.26 arc sec per pixel) covered a 9 arc min by 9 arc min field. Images of the standard stars PG1657+078A, PG1047+003B, and AGK +81° 266 were obtained in order to get photometric calibration. Further observations were acquired with the Bolonia Faint Object Spectrograph and Camera of the Bologna Astronomical Observatory at Loiano, Italy, with the High Resolution Adaptive Camera instrument at the Nordic Optical Telescope (NOT) at La Palma, and again with the WHT on service time on 25–26 August (Table 1).

A comparison among frames acquired on 9 and 10 May allowed us to search for variable objects within the GRB error box, confirming the variability of the object reported by Bond (*10*). This object was inside the x-ray source error box and showed an ultraviolet (UV) excess (Fig. 1), supporting the association of the transient x-ray source with the optical variable. Using aperture photometry software, we determined the magnitudes of the optical transient in all images. About 5 hours after the burst, magnitudes were 20.3 ± 0.3 in the U band and 21.2 ± 0.1 in the R band (*11*). Our optical observations were simultaneous with the BeppoSAX detection of x-ray emission 5.7 hours after the burst, implying a ratio of x-ray (0.5 to 10 keV) to optical luminosity ~10, in contrast to ~200 for GRB 970228.

After an initial phase of constant brightness lasting 1 day [as inferred from the R-band light curve (Fig. 2)], a strong flare took place. The peak brightness of the optical light occurred 2 days after the GRB, and a maximum was reached in the R and U bands at about the same time (Fig. 2). The increase in the brightness of the optical counterpart of GRB 970508 was similar to that inferred for GRB 970228 (*12*), the first burst for which an optical counterpart was identified (*13*). The U- and R-band images taken on 11 May revealed that the source was declining in brightness (*14*). Over the next 3 months, the brightness in the R band declined approximately as a power law (*15*), with the flux $F \propto t^{-1.2 \pm 0.1}$. Our U-band data show that the UV flux declined faster than the flux at longer wavelengths.

An optical spectrum (4300 to 7100 Å) was obtained on 10 May, 21:06 UT, with the 2.2-m CAHA telescope. Data were acquired for only about 300 s, because of the bad weather, and the spectrum had a poor signal-to-noise ratio (S/N). Two spectra obtained on 11 May showed a better S/N ratio. No emission lines were identified in any of the CAHA spectra. The upper limit to the equivalent width is 20 Å (~5×10^{-19} W m^{-2} s^{-1}). Additional spectra were obtained with the Andalucía Faint Object Spectrograph and Camera at the NOT on 16–17 May (Table 2). Metzger and co-workers (*16*) detected an absorption system at redshift $z \sim 0.835$, and consequently, the energy released in GRB 970508 was at least ~10^{44} J s^{-1}. This redshift would also imply that most GRBs, if not all, lie at cosmological distances.

To search for optical variability on time scales of minutes, we obtained 40 images in the B band, with ~1.5 min of time resolution, for ~1 hour on 12 May (04:47 to

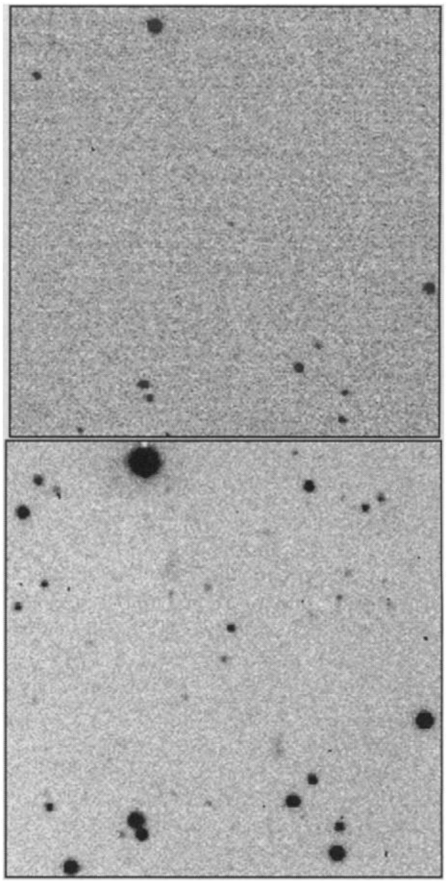

Fig. 1. A 3.0 arc min by 3.0 arc min field containing a fraction of the BeppoSAX GRB error box (*8*), as imaged on 9 May 1997, 02:06 UT, in the U band (upper panel) and 9 May, 03:04 UT, in the R band (lower panel). It contains the full x-ray error box given by the BeppoSAX narrow-field instruments and the location of Bond's variable, at the center of the image. North is at the top, and east is to the left. Limiting magnitudes were ~22 in the U band and ~23 in the R band.

A. J. Castro-Tirado and J. Gorosabel, Laboratorio de Astrofísica Espacial y Física Fundamental, INTA, Madrid, Spain.
N. Benítez and E. Martínez-González, Instituto de Física de Cantabria, Santander, Spain.
C. Wolf, R. Fockenbrock, K. Birkle, Max-Planck-Institut für Astronomie, Heidelberg, Germany.
H. Kristen, A. Broeils, M. Wold, Stockholm Observatory, Saltsjobaden, Sweden.
H. Pedersen, Copenhagen University Observatory, Copenhagen, Denmark.
J. Greiner, Astrophysikalisches Institut, Postdam, Germany.
E. Costa, M. Feroci, L. Piro, Istituto di Astrofisica Spaziale, CNR, Frascati, Italy.
F. Frontera, Dipartimento di Fisica, Università di Ferrara, Ferrara, Italy.
L. Nicastro and E. Palazzi, Istituto Tecnologie e Studio Radiazioni Extraterrestri, CNR, Bologna, Italy.
C. Bartolini, A. Guarnieri, N. Masetti, A. Piccioni, Dipartimento di Astronomia, Università di Bologna, Bologna, Italy.
M. Mignoli, Osservatorio Astronomico di Bologna, Bologna, Italy.
M. Lacy, Nuclear and Astrophysics Laboratory, Keble Road, Oxford, UK.
T. Broadhurst, Department of Astronomy, University of California, Berkeley, CA 94720, USA.
S. Brandt, Los Alamos National Laboratory, Los Alamos, NM 87545, USA.
N. Lund, Danish Space Research Institute, Copenhagen, Denmark.

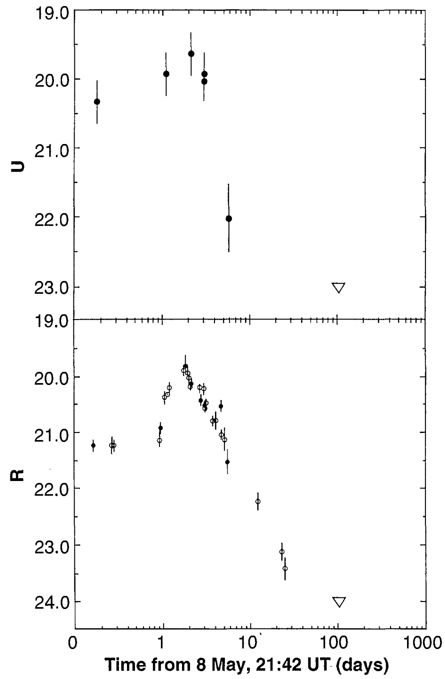

Fig. 2. The U- and R-band light curves of the optical transient related to GRB 970508. Filled circles are data based on our observations obtained at the 4.2-m WHT, 2.5-m NOT, and 2.2-m CAHA telescopes between 9 and 15 May. Empty circles are data from diverse IAU Circulars (*33*). Triangles indicate upper limits obtained on 25–26 August.

05:50 UT) at the WHT. Variability was reported for several kinds of galactic (*17*) and extragalactic (*18*) high-energy transients. However, in the case of the optical transient related to GRB 970508, any variation must have been smaller than 0.2 mag.

Regarding the origin of the optical emission, several models of GRBs predict that the flux density F_ν is proportional to $\nu^{1/3}$ below a critical synchrotron frequency ν_m (*19*). The extrapolation of the gamma ray spectrum leads to a flux density of ~0.02 mJy (1 Jy = 10^{-26} W m^{-2} Hz^{-1}) in the optical band (~20.5 mag), as observed near the peak. However, for GRB 970111, which has been a burst with a fluence one order of magnitude larger, no optical counterpart down to ~0.002 mJy was detected, indicating perhaps some kind of absorption by intervening matter close to the source (*20*).

If we denote the flare amplitude as $\Delta F/F_{\text{initial}}$ and the doubling time scale is defined as $\tau_D = (F_{\text{initial}}/\Delta F)\Delta t$, then $\tau_D \sim 2$ days for the U-band magnitudes observed between 9 and 11 May (20.3 and 19.7, respectively). On 15 May, the U-band magnitude was ~22.0, and on 25 August, ≳23.0; therefore, at quiescence, it is ≳23.0. This value implies that the optical flux had to increase ≳2.5 mag before the first measurement, ~4 hours after the gamma ray event.

Table 2. Journal of the GRB 970508 observations (spectroscopy). The telescope name is preceded by its aperture in meters.

Date of 1997	Time (UT)	Telescope	Integration time (s)	Wavelength range (Å)	S/N
10 May	21:06	2.2 CAHA	~300	4300–7100	~1
11 May	21:29	2.2 CAHA	3600	3500–8000	~10
11 May	22:35	2.2 CAHA	5000	3500–8000	~10
16 May	20:48	2.5 NOT	4800	3650–9100	~2
16 May	22:03	2.5 NOT	4800	4000–10,250	~2
17 May	00:39	2.5 NOT	4800	4000–10,250	~2

There are several explanations for our observations. In the simplest fireball model (*21*), a forward blast wave moves ahead of the fireball and sweeps up the interstellar matter, producing an afterglow at frequencies gradually declining from x-rays to visible and radio wavelengths. The spectrum is then the result of synchrotron radiation (*22*), with a synchrotron break frequency ν_m that is normally in the range 50 keV ≤ $h\nu_m$ ≤ 2 MeV (*h*, Planck constant), although no spectral break was observed in GRB 970508 in the range 20 to 1000 keV, according to BATSE (*7*). In any case, the optical maximum ~2 days after the high-energy event cannot be easily explained by the break frequency moving into the optical band (*23*), and only a more complicated fireball model (*24*) in which the GRB emission is beamed with an initial Lorentz factor of 5 to 10 can account for the observations.

Another prediction of the fireball and afterglow models is that the intensity should rise monotonically before the single maximum in brightness (*25*). In that case, we speculate that another physical mechanism is responsible for the constant phase seen during the first day. In fact, one cannot exclude the presence of optical emission for a few days before the burst. This emission could be, for instance, a consequence of some reservoir of mass being slowly accreted onto a central source, which eventually triggers the burst as a result of some unknown instability, similar to the recurrent x-ray outbursts of some galactic black hole candidates (*26*). A comparable mechanism can work for massive black holes in active galactic nuclei (*27*). The dramatic flare that followed the burst, peaking in ~2 days, could be related to the travel time of the cooling and expanding relativistic fireball debris until it hit a more dense environment, in which the surrounding matter scales as r^{-2}, the inverse square of the radial distance (*28*). In this case, the slope of the light curve should have changed considerably ≤4 hours after the onset of the high-energy event. Then, $\tau_D \leq 0.4$ hours, which is even smaller than $\tau_D \sim 0.7$ hours, as seen in the fastest flare ever detected at UV wavelengths in an extragalactic object (*29*). Another possibility is that optical emission accompanying the x-ray afterglow could have been initially suppressed as a result of synchrotron self-absorption or electron cooling, as predicted by some models (*30*).

The detection of gamma ray bursts at optical wavelengths is improving our understanding of these enigmatic objects. In the future, prompt observations of optical transients related to GRBs will help to clarify the physics during the early optical phase and provide some clues on the nature of the central engine.

REFERENCES AND NOTES

1. For an extensive review of gamma ray burst observations, see G. J. Fishman and C. A. Meegan, *Annu. Rev. Astron. Astrophys.* **33**, 415 (1995).
2. L. Piro, L. Scarsi, R. C. Butler, *Proc. SPIE* **2517**, 169 (1995).
3. F. Frontera *et al.*, *Astron. Astrophys. Suppl. Ser.* **122**, 357 (1997).
4. R. Jager *et al.*, *ibid.* **125**, 557 (1997).
5. E. Costa *et al.*, *IAU Circ. 6649* (1997).
6. J. Heise *et al.*, *IAU Circ. 6652* (1997).
7. C. Kouveliotou *et al.*, *IAU Circ. 6660* (1997).
8. L. Piro *et al.*, *IAU Circ. 6656* (1997); L. Piro *et al.*, *Astron. Astrophys.*, in press.
9. The wide U-band filter that we used was RGO#U8, with a central wavelength of 3557 Å, a half-peak wavelength of 344 Å, and a 74% transmission (M. Broxterman, personal communication).
10. H. E. Bond, *IAU Circ. 6655* (1997).
11. Originally, the U-band results seemed to be in disagreement with those published by T. Galama *et al.* (*31*), but after comparing our data, we agreed on the estimated extinction coefficient value, that is, on the magnitudes of several field stars near the optical transient, and the discrepancy has been removed. See also T. Galama *et al.*, in preparation.
12. A. Guarnieri *et al.*, *Astron. Astrophys.* **328**, L13 (1997); T. Galama *et al.*, *Nature* **387**, 479 (1997).
13. P. J. Groot *et al.*, *IAU Circ. 6584* (1997); J. van Paradijs *et al.*, *Nature* **386**, 686 (1997).
14. A. J. Castro-Tirado *et al.*, *IAU Circ. 6657* (1997); S. Djorgovski *et al.*, *Nature* **387**, 876 (1997).
15. H. Pedersen *et al.*, *Astrophys. J.*, in press.
16. Redshift $z \geq 0.835$ was inferred from Keck spectroscopy on 11 May and 5 June 1997 on the basis of a metal-line absorption system [M. R. Metzger *et al.*, *Nature* **387**, 879 (1997)] and a faint [O II] emission line (*32*).
17. G. M. Beskin *et al.*, in *Flares and Flashes*, J. Greiner, H. W. Duerbeck, R. E. Gershberg, Eds. (Lecture Notes in Physics 454, Springer, Berlin, 1995), pp. 330–333.
18. A 1-hour-long flare with a rise of 0.46 mag in 32 min and a very rapid decline of 0.52 mag in 10 min was observed in the B band for the BL Lac object 3C 66A [G. Z. Xie *et al.*, *Astron. Astrophys. Suppl. Ser.* **106**, 361 (1994)].
19. J. I. Katz, *Astrophys. J.* **432**, L107 (1994).
20. A. J. Castro-Tirado *et al.*, *IAU Circ. 6598* (1997);

J. Gorosabel *et al.*, in preparation.
21. P. Mészáros and M. J. Rees, *Astrophys. J.* **405**, 278 (1993); *ibid.* **418**, L59 (1993).
22. ———, *ibid.* **476**, 232 (1997).
23. The impulsive fireball model in (*22*) predicts that the observed break frequency ν_m crosses the optical band at a time $t_{op} \sim 3 \times 10^3\ t_\gamma$, where t_γ is the duration of the gamma ray flash. Taking into account that the bulk of the GRB 970508 gamma ray emission lasted 3.6 s, $t_{op} \sim 3$ hours, which is much shorter than the observed $t_{op} \sim 2$ days.
24. R. A. M. J. Wijers, M. J. Rees, P. Mészáros, *Mon. Not. R. Astron. Soc.* **288**, L51 (1997)
25. J. I. Katz and T. Piran, *Astrophys. J.* **490**, 772 (1997); and references therein.
26. Like GRO J0422+32 [A. J. Castro-Tirado, J. L. Ortiz, J. Gallego, *Astron. Astrophys.* **322**, 507 (1997)] and GRO J1655-40 [J. A. Orosz, R. A. Remillard, Ch. D. Bailyn, J. E. McClintock, *Astrophys. J.* **478**, L83 (1997)].
27. S. K. Chakrabarti and P. J. Wiita, *Astrophys. J.* **411**, 602 (1993). See also J. J. Brainerd, *ibid.* **394**, L33 (1992).
28. M. Vietri, *ibid.* **488**, L105 (1997).
29. The fastest x-ray flare ever seen in an extragalactic object was observed in May 1994 in the BL Lac object PKS 2155-304. The x-ray flare was followed by a broader, lower amplitude extreme-UV flare ~1 day later and a broad, low-amplitude UV flare ~2 days later [E. Pian *et al.*, *Astrophys. J.* **486**, 784 (1997)].
30. M. Tavani, *Astrophys. J.* **466**, 768 (1996); E. Waxman, *ibid.* **485**, L5 (1997).
31. T. Galama *et al.*, *IAU Circ. 6655* (1997).
32. M. R. Metzger *et al.*, *IAU Circ. 6676* (1997).
33. S. Djorgovski *et al.*, *IAU Circ. 6658* (1997); *IAU Circ. 6660* (1997); B. Schaefer *et al.*, *IAU Circ. 6658* (1997); P. Groot *et al.*, *IAU Circ. 6660* (1997); C. Chevalier and S. Ilovaisky, *IAU Circ. 6663* (1997); A. Kopylov *et al.*, *ibid.*; *IAU Circ. 6671* (1997); A. Fruchter and L. Bergeron, *IAU Circ. 6674* (1997); (*31, 32*).
34. We are grateful to M. Santos-Lleó, M. Más-Hesse, B. Montesinos, P. Rodríguez-Pascual, L. Sánz Fernández de Córdoba, E. Fernandes-Vieira, J. R. Acarreta, A. Alberdi, M. Cerviño, T. Galama, N. Schartel, D. Thompson, and R. Wijers for fruitful conversations, and to J. Gallego, J. Zamorano, and M. Fernández for their good will. We are grateful to the director of NOT for his continued support of this program, and to J. Perez-Mercador for his encouragement. J. Greiner is supported by the Deutsche Agentur für Raumfahrtangelegenheiten. C.B., A.G., N.M., and A.P. acknowledge the support of the Università di Bologna. The BeppoSAX team acknowledges the Italian Space Agency for support. The Calar Alto German-Spanish Observatory is operated jointly by the Max-Planck Institut für Astronomie in Heidelberg and the Comisión Nacional de Astronomía, Madrid. The WHT is operated by the Royal Greenwich Observatory in the Spanish Observatorio del Roque de los Muchachos of the Institutò de Astrofísica de Canarias. The Loiano Telescope is operated by Osservatorio Astronomico di Bologna and Università di Bologna.

24 June 1997; accepted 14 January 1998

Temperature and Surface-Ocean Water Balance of the Mid-Holocene Tropical Western Pacific

Michael K. Gagan, Linda K. Ayliffe, David Hopley, Joseph A. Cali, Graham E. Mortimer, John Chappell, Malcolm T. McCulloch, M. John Head

Skeletal Sr/Ca and $^{18}O/^{16}O$ ratios in corals from the Great Barrier Reef, Australia, indicate that the tropical ocean surface ~5350 years ago was 1°C warmer and enriched in ^{18}O by 0.5 per mil relative to modern seawater. The results suggest that the temperature increase enhanced the evaporative enrichment of ^{18}O in seawater. Transport of part of the additional atmospheric water vapor to extratropical latitudes may have sustained the $^{18}O/^{16}O$ anomaly. The reduced glacial-Holocene shift in seawater $^{18}O/^{16}O$ ratio produced by the mid-Holocene ^{18}O enrichment may help to reconcile the different temperature histories for the last deglaciation given by coral Sr/Ca thermometry and foraminiferal oxygen-isotope records.

Oxygen isotopes in foraminifera from deep-sea cores have been used successfully to reconstruct continental ice volumes, glacio-eustatic sea level, and deep-ocean temperatures throughout the last glacial-interglacial cycle (*1*). Yet there is still considerable debate regarding the relative contributions of changes in the oxygen isotopic composition of seawater and ocean temperature to the change in foraminiferal $\delta^{18}O$ values (*2*) in the tropical surface ocean. The amplitude of the glacial-Holocene $\delta^{18}O$ shift for planktonic foraminifera in the tropics is about the same as that for foraminifera living in the near-constant temperature environment of the deep ocean (*3*). The apparent similarity between the two records has led to the interpretation that the tropical surface ocean cooled by no more than 2°C during the last glacial maximum (LGM), an interpretation reinforced by the conclusions of the CLIMAP project (*4*). Recent measurements of Sr/Ca ratios in corals from Barbados (*5*) and Vanuatu (*6*) indicate that both the tropical Atlantic and Pacific oceans cooled by up to 5°C during the LGM. Despite the consistency of this cooling with the 5°to 8°C cooling estimated for the tropical atmosphere (*7*), the coral records have not been widely accepted because the glacial-Holocene $\delta^{18}O$ shift recorded by planktonic foraminifera cannot accommodate an ocean temperature shift of 5°C, particularly in the tropical Pacific where the $\delta^{18}O$ shift is anomalously small (*8*). If the coral Sr/Ca thermometer is reliable, the relatively small $\delta^{18}O$ shift for Pacific planktonics may be a result of undetected changes in the distribution of ^{18}O in the surface ocean (*9*). Therefore, obtaining accurate estimates of the past ^{18}O distribution in tropical surface waters, by some independent means, is crucial to establishing the role of the tropical oceans in global climate change.

In principle, precise measurements of Sr/Ca ratios and $\delta^{18}O$ values in coralline aragonite should make it possible to determine uniquely the past oxygen isotopic composition of seawater, by removal of the temperature component of the coral $\delta^{18}O$ signal. However, the temperature dependence of coral Sr/Ca ratios has been questioned recently (*10*) on the basis that biological controls on Sr and Ca uptake can induce uncertainties of up to 3°C in reconstructed temperatures. Here, we first verify the reliability of the coral Sr/Ca thermometer for several modern corals growing in suboptimal environmental settings like those that may prevail during glacial-interglacial transitions when corals colonize transient shorelines marked by fluctuations in temperature, salinity, and water turbidity. Next we demonstrate a strong correlation between coral Sr/Ca and $\delta^{18}O$ and, by coupling these measurements, determine the surface temperature and $\delta^{18}O$ of western Pacific seawater soon after the end of the last deglaciation. Interpretations of the glacial-Holocene shift in foraminiferal $\delta^{18}O$ have been made with the assumption that the ^{18}O distribution in the surface ocean was the same as today at ~6000 years before the present, by which time the discharge into the ocean of ^{18}O-depleted polar meltwater was essentially complete (*11*). We test this assumption by analyzing a 5350-year B.P. coral from the Great Barrier Reef.

We measured skeletal Sr/Ca (*12*) for colonies of *Porites lutea* growing in three different oceanic environments including the Great Barrier Reef, the eastern Indian Ocean, and the Indonesian seaway. These test sites encompass seasonal sea surface temperature (SST) ranges (20° to 31°C) spanning much of the survival range for

M. K. Gagan, L. K. Ayliffe, J. A. Cali, G. E. Mortimer, M. T. McCulloch, Research School of Earth Sciences, Australian National University, Canberra, ACT 0200, Australia.
D. Hopley, Sir George Fisher Centre, James Cook University, Townsville, Queensland 4811, Australia.
J. Chappell and M. J. Head, Research School of Pacific and Asian Studies, Australian National University, Canberra, ACT 0200, Australia.